Day-1 INSAT-3DR Vicarious Calibration Using Reflectance-Based Approach Over Great Rann of Kutch

Piyushkumar N. Patel, K. N. Babu, R. P. Prajapati, Vikram Sitapara & A. K. Mathur

Journal of the Indian Society of Remote Sensing

ISSN 0255-660X

J Indian Soc Remote Sens
DOI 10.1007/s12524-017-0729-z

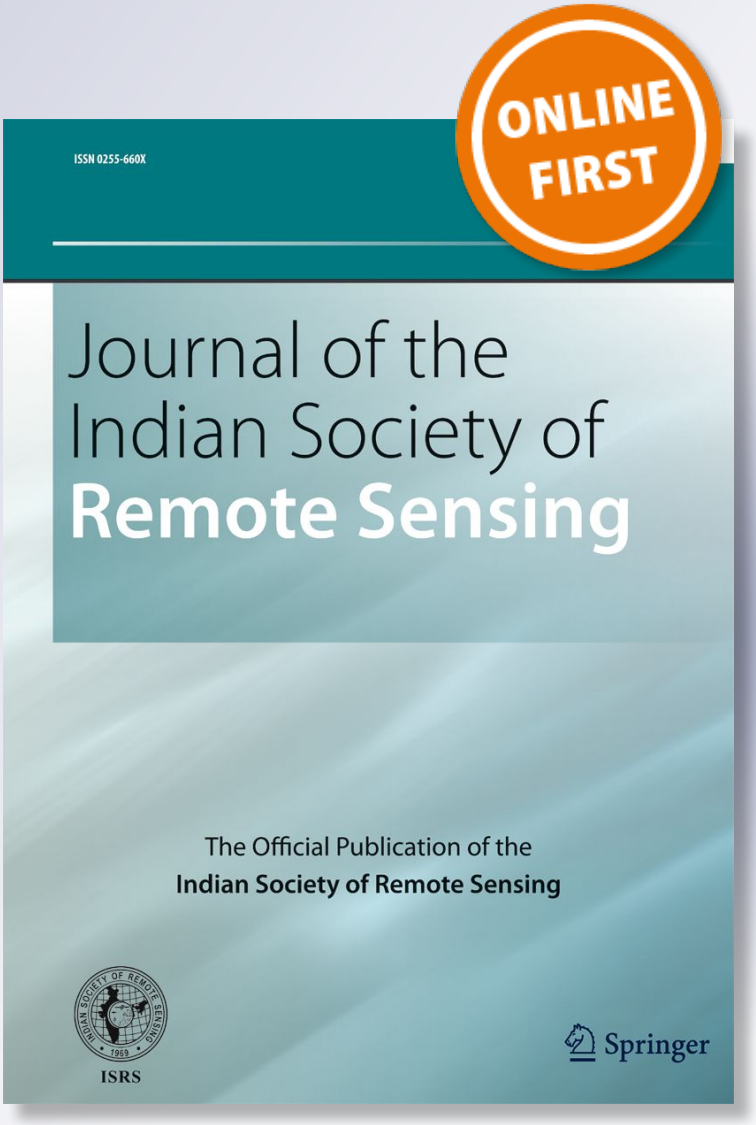

Springer

Journal of the Indian Society of Remote Sensing
https://doi.org/10.1007/s12524-017-0729-z

RESEARCH ARTICLE

Day-1 INSAT-3DR Vicarious Calibration Using Reflectance-Based Approach Over Great Rann of Kutch

Piyushkumar N. Patel[1] · K. N. Babu[1] · R. P. Prajapati[1] · Vikram Sitapara[1] · A. K. Mathur[1]

Received: 14 July 2017 / Accepted: 13 November 2017

Abstract
This study describes the post-launch calibration for visible (VIS) and shortwave infrared (SWIR) bands of Indian National Satellite System (INSAT)-3DR imager over Great Rann of Kutch (GROK) on Day-1 (15th September 2016), when the first time INSAT-3DR Imager camera was switched on. In order to account the characterization of errors and undetermined post-launch changes in sensor spectral response, this calibration activity was performed and extended for its monitoring to Day-56 (since the Day-1; 09th November 2016). A reflectance based technique is used in the present study. The surface reflectance and atmospheric variables were measured over the site as per solar and viewing geometry of the INSAT-3D scan. Top of atmosphere (TOA) spectral radiances were computed using 6SV (second simulation of the satellite signal in the solar spectrum) radiative transfer code with the in situ measurements as well as spectral response function of each channel. Preliminary results of the Day-1 vicarious calibration yield gain coefficients of 0.974 and 0.820 for VIS and SWIR channels respectively despite the inhomogeneity of the ground target caused by sufficient sub-surface soil moisture. In extension of the present study, the obtained gain coefficients were 1.001 and 0.9887 for VIS and SWIR, respectively, during Day-56 which indicates the performance of sensor is within the range of pre-launch laboratory calibration.

Keywords INSAT-3DR · Vicarious calibration · Reflectance · 6SV · Radiative transfer model

Introduction

The advancement and popularity of satellite data usage for societal benefits not only requires the development of new and complex satellites but also to improve the quality of satellite sensors and their data products. Therefore, it has become more essential to continually upgrade the ability to provide calibration of sensors. Generally, calibration procedure includes first radiometric calibration prior to the launch (Bruegge et al. 1998) and later the on-board calibration (Bruegge et al. 1993), but in the absence of on-board calibration facility, a post-launch vicarious calibration exercise provides an aid to compensate the degradation of the satellite sensor (Rao 2001). Vicarious calibration provides a method for calibration of satellite sensors using reference and precise measurements of spectral reflectance from the ground instruments over a terrestrial calibration site. This calibration coefficients can be incorporated for the accurate characterisation of the conversion of digital counts to radiance values. Vicarious calibration is a broadly adopted technique for continuous monitoring the radiometric performance of satellite sensor, which involves the uncertainties computation in the calibration coefficients to correct the radiometric response of the sensor (Thome et al. 1998). Vicarious calibration is performed with radiance simulation using measured ground reflectance and atmospheric parameters on clear day with less aerosol conditions to those at the satellite level.

INSAT-3DR is an advanced weather satellite of India configured with improved imaging system and atmospheric sounder as compare to earlier Indian National Satellite System (INSAT) missions like INSAT-3A and KALPANA-1. Vicarious calibration is performed to monitor the in-orbit performance of VIS and SWIR channels of INSAT-3DR imager on day-1 at 1130 Indian Standard Time (IST) (15th September 2016), i.e. when the first time INSAT-3DR VIS (0.55–0.75 μm) and SWIR

✉ Piyushkumar N. Patel
piyushether@gmail.com

[1] Calibration and Validation Division, Space Applications Centre, ISRO, Ahmedabad, India

Published online: 06 January 2018

(1.55–1.70 μm) camera was switched-on and the study was extended to Day-56 (9th November 2016). The reflectance-based approach is used with in situ measurements of surface reflectance and atmospheric parameters for the vicarious calibration exercise. The 6SV radiative transfer (RT) code is used to estimate the TOA spectral radiance using ground measured parameters along with pre-launch laboratory measured spectral response function (SRF). The 6SV simulated TOA spectral radiances were compared with the INSAT-3DR measured TOA spectral radiance to estimate the calibration coefficients of each channel. The uncertainties involved in the computation due to model, surface measurements, variation in aerosol types and surface anisotropic effect were also estimated for both the channels of INSAT-3DR and are discussed in subsequent sections.

INSAT-3DR Specifications

The Indian National Satellite System (INSAT-3DR) is the multipurpose satellite which provides meteorological, television broadcasting, telecommunication and search and rescue services. INSAT-3D and INSAT-3DR are the advanced meteorological satellites, aiming for a significant technological improvement in sensor capabilities as compared to earlier INSAT satellites series. INSAT-3DR satellite was launched successfully on 8th September 2016 using a GSLV MK-II launch vehicle from SDSC–SHAR–ISRO. It is equipped with a 6-channels Imager and a 19-channels atmospheric sounder, which operate in visible to thermal infrared region of the electromagnetic spectrum. INSAT-3DR imager operates from a geostationary altitude of 36,000 km in visible (VIS) and short wave infra-red (SWIR) bands with 1 km spatial resolution, while mid-wave infra-red (MWIR), thermal infra-red 1 (TIR1), thermal infra-red-2 (TIR2) and water vapor (WV) bands with 4 km spatial resolutions. INSAT-3DR sounder has 18 Infrared (IR) channels ranging from 3.7 to 14.7 μm and one visible channel for the cloud detection during daytime with a 10-km spatial resolution. The significant improvements incorporated in INSAT-3DR are: (1) imaging in MWIR band to provide nighttime pictures of low clouds and fog and (2) imaging in the split band TIR channel with two separate windows (10.2–11.2 and 11.5–12.5 μm regions) with 4 km spatial resolution provides estimation of sea surface temperature with better accuracy. INSAT-3DR radiance calculation and estimation of calibration coefficients are similar to previously launched INSAT series satellite INSAT-3D and details are provided in Patel et al. (2016).

Test Site and Field Measurements

Calibration Site

Attributing to their preferable stability of surface characteristics and atmospheric dynamics, pseudo-invariant sites are commonly used for sensor radiometric calibration, degradation monitoring and inter-comparisons (Chander et al. 2010; Bouvet 2014) especially for the satellite sensors without on-board calibration facilities. The Committee on Earth Observation Satellites (CEOS) Working group on Calibration and Validation identified several sites around the world (Teillet and Chander 2010) based on certain selection criteria, such as low probability of atmospheric variability, high spatial homogeneity, weak directional effects, flat reflectivity spectrum. Calibration sites are never chosen randomly, and to be adequate they must satisfy a certain number of criteria (Scott et al. 1996; Slater et al. 1996, 1987; Teillet et al. 1997). Based on these criteria, we have selected a desert site in Great Rann of Kutch (GROK) (23.67°N and 69.66°E and $\sim$ 4 *m above mean* sea level), Gujarat. This calibration site is extended up to $\sim$ 10 km square area, presenting a flat and homogenous terrain characterized by a low surface reflectance (observed during Day-1 campaign) with high soil moisture content due to excessive water logging during the monsoon season. Figure 1 indicates the observational site in Great Rann of Kutch for the vicarious calibration of INSAT-3DR. The site is a clay-dominated dry land with different spectral characteristics that have been used for radiometric calibration sites for large footprint sensors (e.g. INSAT-3DR, INSAT-3D and INSAT-3A) (Patel et al. 2014, 2016).

Field Campaign

Measurements of ground reflectance were carried out with a spectroradiometer (FieldSpec 3, Analytical Spectral Devices (ASD), Inc.), which covers the spectral range from 350 to 2500 nm and were made at random sampling points covering over a region of 4 km^2. On ground, data was collected centre over 1130 IST on Day-1 for a period of 1 h and during 1000–1300 h IST for the Day-56 to cover five INSAT-3DR scans. Total 30 and 60 spectra of ground reflectance were covered within a 2 × 2 km site during Day-1 and Day-56, respectively.

Figure 2 shows the measured surface reflectance over the calibration site for Day-1 and Day-56 along with standard deviation (at 1σ level). Small boxes at the bottom panel illustrates the variation of reflectance corresponding to INSAT-3DR bands. Water vapor absorption at 1380 nm and 1800 nm are the major reasons for the observed two gaps in the reflectance curves. The standard deviation of

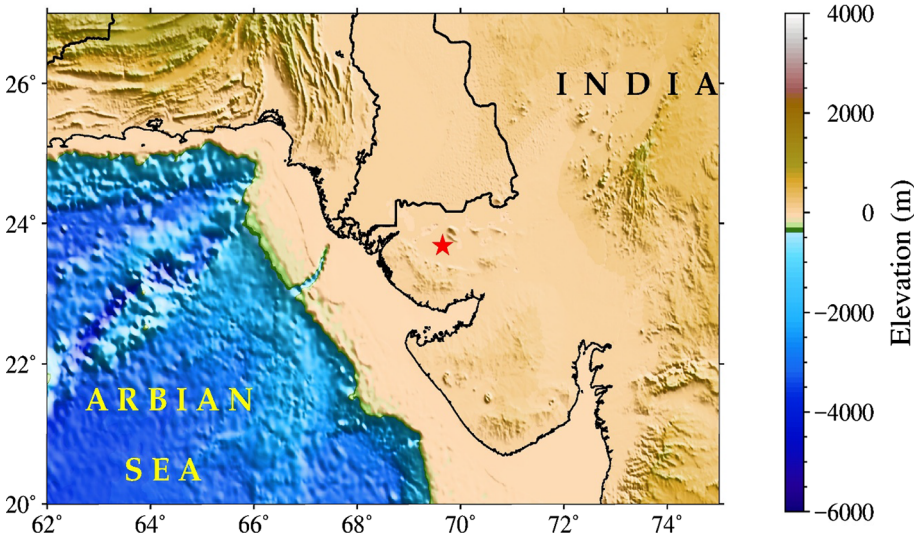

Fig. 1 Location of calibration site (in solid red-star) at Great Rann of Kutch (GROK), Gujarat (color figure online)

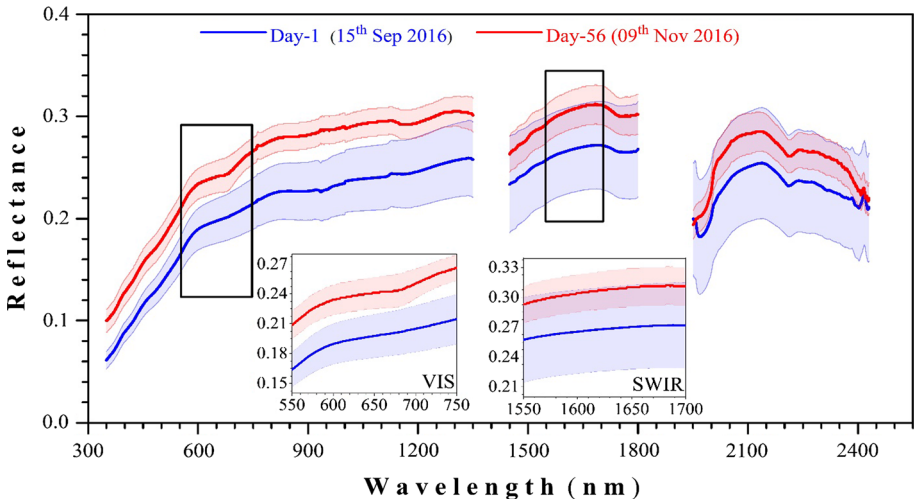

Fig. 2 Measured surface spectral reflectance on Day-1 (in blue) and Day-56 (in red) over observational site. Solid color lines indicate the mean value and shaded portion indicates the spectral standard deviation among all the measurements. The small boxes refer to the reflectance spectra for the corresponding INSAT-3DR wavebands (color figure online)

the measured reflectance was observed to be 3 and 8% for VIS and SWIR bands respectively on Day-1, whereas it reduced to 1.9 and 3% on Day-56, which indicates the minor spatial variation and uniformity of site.

The aerosol optical depth (AOD) measurements were carried out using a multiwavelength Microtops-II sunphotometer (Solar Light Co., USA) at five different wavelengths at 380, 440, 500, 675 and 870 nm, from the solar instantaneous flux measurements with its internal calibration using the Langley method (Reagan et al. 1986; Schmid and Wehrli 1995). The Full Width at Half Maximum (FWHM) bandwidth for the 380 nm channel is 2.4 ± 0.4 and 10 ± 1.5 nm for the other channels (Morys et al. 2001). A Microtops-II Ozonometer, a ground-based instrument, which is capable of measuring the total column ozone (TCO) using three UV channels (305.5, 312.5, 320.0 nm) and the total water vapor content (WVC) using two near-IR channels (940 and 1020 nm) (Porter et al. 2001) as well as AOD at 1020 nm was also used to measure atmospheric variables. Table 1 contains the hourly value of AOD at 500 nm, TCO and WVC over GROK for Day-1 and Day-56. More details of design, performance, error and calibration of Microtops-II is given elsewhere (Porter et al. 2001; Morys et al. 2001; Badarinath et al. 2007).

Site Characteristics

Radiometric spatial uniformity and temporal stability of targets are the main features to be considered for calibration site selection along with long-term radiometric control of satellite sensor data (Bannari et al. 2005; Cosnefroy et al. 1996; Gu et al. 1990; Rondeaux et al. 1998). The optical characteristics of any target site can vary due to topography variation, soil moisture variation, cracks in the dry surface that trap light, presence of vegetation, non-Lambertian behaviour of the surface increasing BRDF effects, as well as meteorological conditions. (Frouin and

Table 1 Hourly mean values of atmospheric variables, i.e. AOD at 500 nm, total columnar ozone and columnar water vapor over Great Rann of Kutch (GROK) during Day-1 and Day-56

Date	Hours (IST)	AOD at 500 nm	Total columnar ozone (DU)	Water vapor content (g cm^{-2})
Day-1 (15th Sep 2016)	1130	0.385	302	2.30
Day-56 (09th Nov 2016)	1014	0.209	280	0.85
	1044	0.217	275	0.81
	1114	0.225	272	0.79
	1144	0.221	270	0.78
	1214	0.223	271	0.76

Gautier 1987; Scott et al. 1996; Slater et al. 1996; Teillet et al. 1997; Thome 2001). Radiometric spatial uniformity of the calibration site is ascertained by calculating spatial Coefficient of Variation (CV) using cloud-free INSAT-3DR radiances over the site during Day-1 and Day-56.

VIS and SWIR bands radiance data for Day-1, 1130 IST and Day-56 1144 IST were analysed to compute CV. CV is defined by the ratio of the standard deviation and the average of the radiances. In order to characterize the variability of the spatial homogeneity of the site, we set a 2 km × 2 km window size with a sampling step of 1 km. Figure 3 illustrates the result obtained using an INSAT-3DR images acquired on Day-1, 1130 IST and Day-56 1144 IST with the data collected site (2 km × 2 km) in black box. The mean CV was found to be similar for VIS bands during Day-1 (3.1%) and Day-56 (2.9%), whereas a significant change in CV was observed for the SWIR band on Day-1 (5.5%) and Day-56 (3.9%). The substantial variation in CV for the SWIR band indicates temporal inhomogeneity of the ground surface induced by sufficient sub-surface soil moisture due to excessive water logging during the monsoon season.

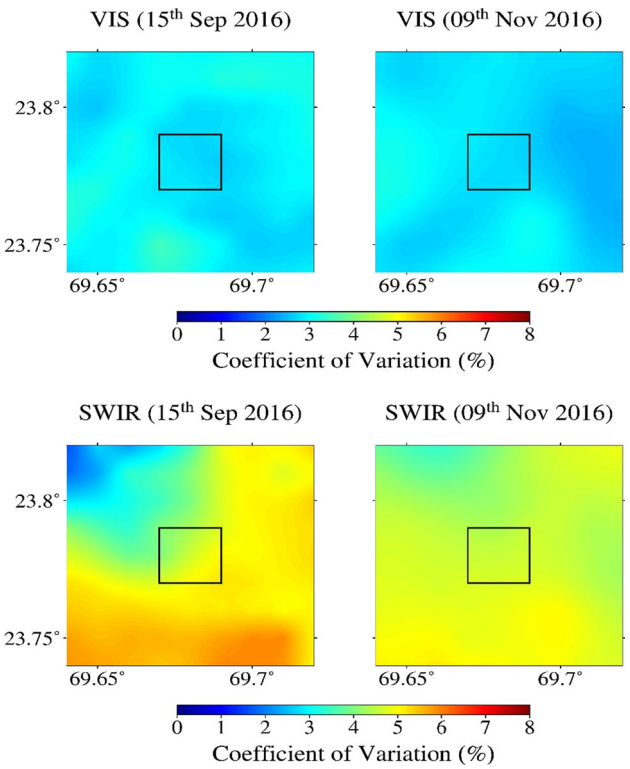

Fig. 3 Images of the computed coefficient of variation (CV) using 2 km × 2 km window in the two bands (VIS and SWIR) of a INSAT-3DR image acquired over GROK on Day-1;1130 h and Day-56;1144 h. Black box shows the data collection site

Methodology

It is difficult to maintain the radiometric accuracy of the spectral radiometer that measures the surface radiance in the radiance-based technique, therefore we have adopted the reflectance-based technique in the present study (Slater et al. 1987). The reflectance-based technique mainly depends on measured ground surface reflectance. The reflectance is characterized by the ratio of measured reflectance over the site to a standard reflectance of spectralon panel for which the bidirectional reflectance factor is precisely determined. The vicarious radiometric calibration depends on the surface reflectance and radiance from the sun to earth's surface and earth's surface to sensor and atmospheric optical thickness over the calibration site at the time of satellite over pass. The ground measurements are used as an input for radiative transfer (RT) model to simulate the at sensor radiances for the required bands. The ground measurements are used to define the spectral directional reflectance of the surface, the spectral optical depth that are used to describe the aerosol and molecular scattering effect in the atmosphere (Gellman et al. 1991) and along with this we also used columnar water vapor to include the water vapor absorption effect. We have used improved 6SV RT code (Vermote et al. 2006; Kotchenova et al. 2008) to compute the radiance field using ground measurements. 6SV RT code predicts the satellite signal at TOA level using ground reflectance measurements and

atmospheric measurements using sunphotometer. 6SV RT model is physics based model, which is not specified for particular satellite or test sites. Because of that 6SV RT model is used for this study. In addition, 6SV RT model has covered gaseous absorption and scattering by aerosols and molecules. 6SV deals better with atmospheric scattering than other RT models (Markham et al. 1992). 6SV model was formulated for the atmospheric correction in the short wavelengths of electromagnetic spectrum. 6SV code requires the geometric conditions (viewing zenith, viewing azimuth, solar zenith and solar azimuth angles). The sensor viewing zenith and azimuth angles are obtained from INSAT-3DR metadata files and solar zenith and azimuth angles are calculated using date, time and location of field measurement. Figure 4 describes the detailed work flow for the simulation of TOA radiance and estimation of calibration coefficient.

During the vicarious calibration exercise, the selection of optimum aerosol type plays an important role. The actual aerosols characteristics were often very different compare to those of the standard aerosol models in the RT codes. It is difficult to precisely estimate the aerosol characteristics in the field campaign. This may lead to a systematic error in calibration results (Chen et al. 2014). In this study, continental aerosol model along with desert and urban aerosol model were used in order to approximate their contributions to the systematic calibration uncertainty as the results are close to the satellite observations and therefore considered for further discussion.

We have used pre-launch laboratory measurements of spectral response function (SRF) of INSAT-3DR VIS and SWIR channels (Fig. 5) of Imager as an input to the RT code to compute TOA radiances. Both the SRF and ground reflectance data are resampled to 2.5 nm intervals using a spline interpolation method. 6SV RT model provides an output in the form of TOA radiance, which is divided by the corresponding radiance observed by the INSAT-3DR for particular channel to yield calibration coefficients.

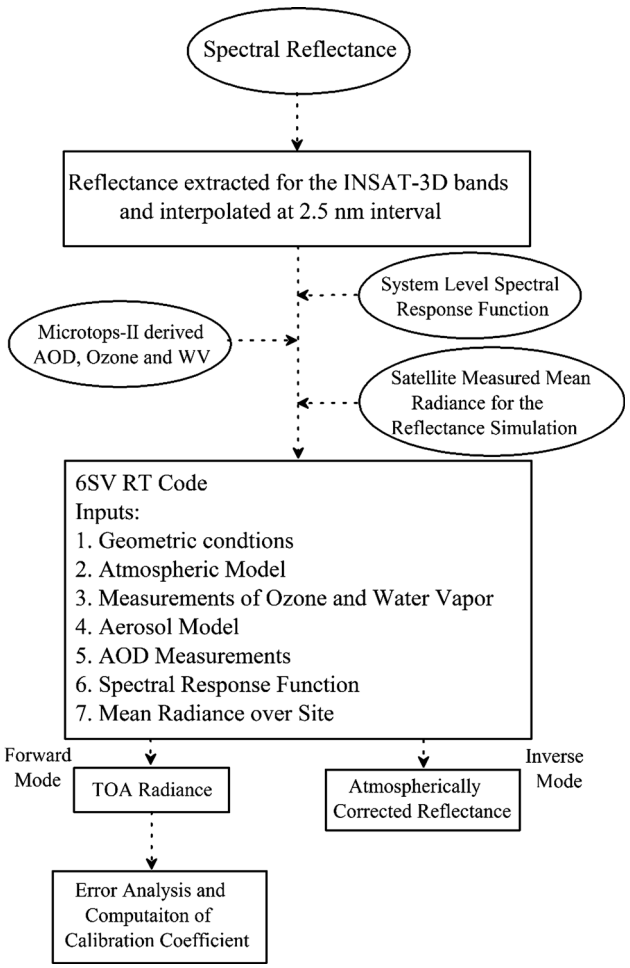

Fig. 4 Work flow for the simulation of TOA radiance and estimation of calibration coefficient

Analysis of BRDF Effect

Surface albedo is related to surface reflectance which depends on the bidirectional reflectance distribution function (BRDF), which indicates the dependence of reflectance on solar and viewing geometry (Nicodemus et al. 1977). In general, reflectance of light is an anisotropic phenomenon and this anisotropy is very small as compared to the Lambertian component except at special geometries like specular reflection from water surface. The precise computation of surface reflectance requires the anisotropy estimation. The BRDF effect provides a precise computation of uncertainty in reflectance arising due to evading the anisotropy component. We provided this BRDF effect into 6SV simulation using MODIS derived BRDF product (MCD43A1) (http://lpdaac.usgs.gov/product/modis/mod43a1), which is a combined MODIS Terra and Aqua product. The MCD43A2 data product (MODIS ATBD 1999) provides high quality three Ross-Li BRDF model parameters (isotropic, volume scattering and geometric optical reflectance terms), which were pixel-wise implemented into 6SV RT model to estimate BRDF effect. We used approximately common bands for MODIS and INSAT-3DR. MODIS provides BRDF coefficients in the seven narrow bands and three broad bands. We have used MODIS first broad band (0.4–0.7 μm) for VIS (0.55–0.75 μm) channel of INSAT-3DR imager and MODIS SWIR band (1.628–1.652 μm) for SWIR band (1.55–1.70 μm) of INSAT-3DR imager. In order to estimate the impact of BRDF on TOA radiance, 6SV RT model was run with and without BRDF. BRDF impact on TOA radiances is discussed further in the following subsection of "Error Analysis and Budget".

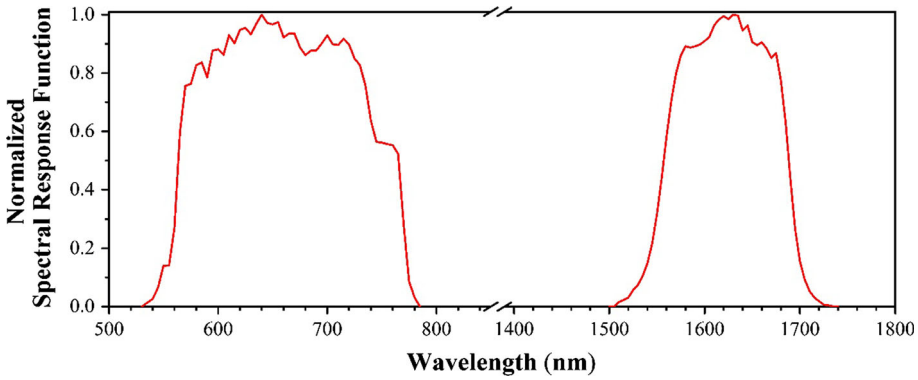

Fig. 5 Pre-launched laboratory measurements of spectral response function for VIS and SWIR bands of INSAT-3DR imager

Results and Discussion

To perform the vicarious calibration for the two bands of INSAT-3DR over GROK, the 6SV simulated TOA spectral radiance is compared with INSAT-3DR measured radiance.

Radiance Comparison

Table 2 shows the detailed mean values of simulated and satellite observed radiance along with calibration coefficients and relative error in measurements. As the INSAT-3DR imager camera was switched on to acquire a single image at 1130 on Day-1, the comparison of satellite observed and simulated TOA radiance are discussed further in Table 2. The comparative analysis for Day-1 indicates that the satellite observed radiance value (81.88 W m^{-2} sr^{-1} μm^{-1}) is very well agreed with the simulated radiance (79.73 W m^{-2} - sr^{-1} μm^{-1}) in the VIS channel, which shows uniformity of the site for the VIS channel. On the other hand, the large difference was observed between INSAT-3DR (18.87 W m^{-2} sr^{-1} μm^{-1}) and simulated radiance (15.47 W m^{-2} sr^{-1} μm^{-1}) values in the SWIR channel indicating inhomogeneity due to sub-surface soil moisture content, which is clearly seen in the analysis of coefficient of variation (Fig. 3).

Figure 6 shows the result of regression of TOA radiance for VIS and SWIR bands of INSAT-3DR imager for the Day-56. In order to reduce the geolocation error, we have averaged the data on hourly basis and compared with the satellite observations. The result indicates a good statistical agreement between INSAT-3DR derived and 6SV simulated TOA radiance with R^2 values of 0.987 and 0.938 for VIS and SWIR, respectively. The estimated RMSE values are found to be very small, 0.40 and 0.47 W m^{-2} sr^{-1} - μm^{-1} for VIS and SWIR respectively. The large RMSE in SWIR channel still indicates the influence of soil moisture but it is improved from Day-1. The bias between satellite derived radiance and 6SV simulated radiance are observed very minimal, with the values of 0.10 and

Table 2 Summary of INSAT-3DR observed and 6SV simulated radiance along with calibration coefficients and relative error for Day-1 and Day-56

Day/hour (IST)	Channels	INSAT-3DR radiance (W m^{-2} sr^{-1} μm^{-1})	6SV simulated radiance (W m^{-2} sr^{-1} μm^{-1})	Relative errors in radiance (%)	Calibration coefficient
Day-1/1130	VIS	81.88	79.73	− 2.62	0.974
	SWIR	18.87	15.47	− 18.01	0.820
Day-56/ 1044	VIS	77.28	78.05	0.99	1.009
	SWIR	15.26	15.06	− 1.31	0.986
Day-56/ 1114	VIS	79.43	79.28	− 0.18	0.998
	SWIR	16.72	16.52	− 1.19	0.988
Day-56/ 1144	VIS	84.03	83.78	− 0.29	0.997
	SWIR	17.72	18.18	2.59	1.026
Day-56/ 1214	VIS	85.25	85.45	0.23	1.002
	SWIR	19.36	18.83	− 2.73	0.972
Day-56/ 1244	VIS	84.94	84.90	− 0.04	0.999
	SWIR	18.89	18.32	− 3.01	0.970

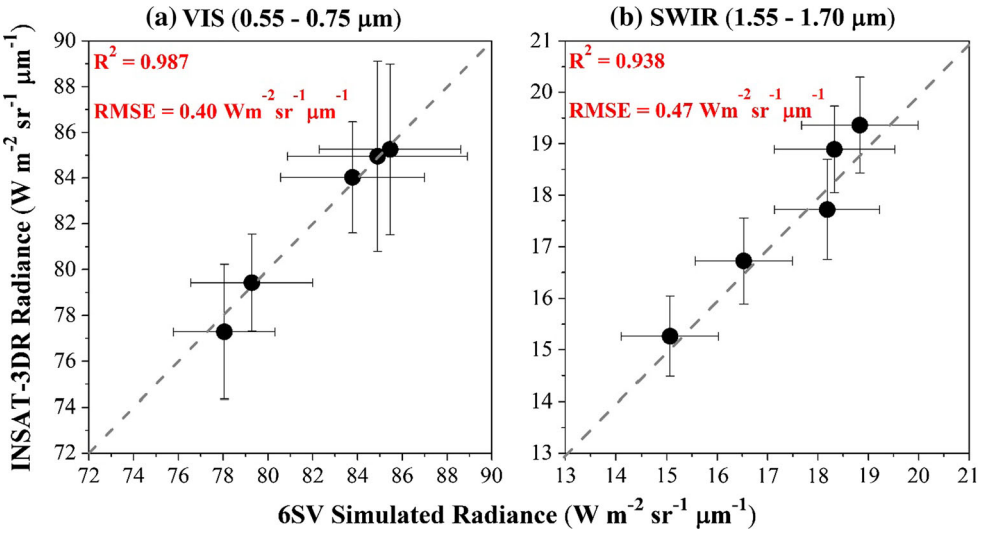

Fig. 6 Comparison between INSAT-3DR observed TOA radiance and 6SV simulated TOA radiance for **a** VIS and **b** SWIR channels on Day-56 over GROK

0.20 W m^{-2} sr^{-1} μm^{-1} for VIS and SWIR bands respectively. On average, relative error (RE) between the 6SV simulated and INSAT-3DR derived radiances are 0.13 and − 1.1% for VIS and SWIR, respectively, which indicates that the INSAT-3DR imager slightly underestimates the radiance values by 0.13% in VIS and overestimates by 1.1% in SWIR band. The correlation is found better in SWIR on Day-56 compared to Day-1. The standard deviation of the radiance values in Fig. 6 indicates the hourly spatial variation of site both from INSAT-3DR and 6SV.

Vicarious Calibration Coefficient

The vicarious calibration coefficient is the ratio of 6SV simulated radiance and satellite observed radiance. For an ideal case, if there is no degradation in the sensor during launch and if the ground and atmosphere were properly characterized and the RT code is perfect then simulated TOA radiance should precisely match with satellite observed radiance. It means that the ratio of simulated to observe radiance should be unity. In practice it is not possible, there are uncertainties in field reflectance and atmospheric measurements, and RT modelling uncertainties. To evaluate the coefficients and describe the characteristics of INSAT-3DR observed radiance, we compared the vicarious calibration coefficients derived for VIS and SWIR (Fig. 7) for Day-1 and Day-56. The result shows a small deviation in calibration coefficients from unity for VIS channels of INSAT-3DR imager, whereas the deviation from unity in SWIR channels during Day-1 clearly indicates the large contribution of sub-surface soil moisture. The standard deviation in calibration coefficients is found to be less than 2% for Day-56 for each band indicates stability of the satellite performance. The mean calibration coefficients are found to be 1.001 and 0.988 for

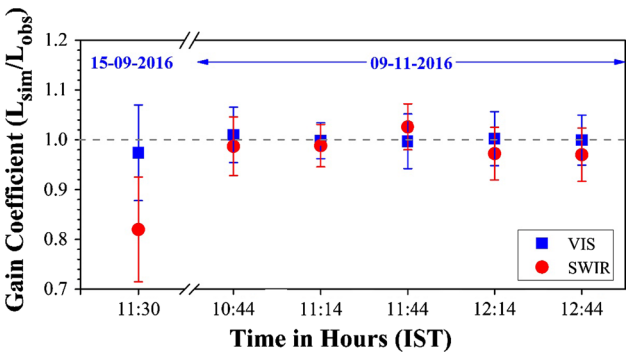

Fig. 7 Variation of estimated gain coefficients using vicarious calibration both for VIS and SWIR channels of Day-1 and Day-56

VIS and SWIR, respectively for Day-56. The differences between simulated and observed radiance are very small and which is due to the intrinsic variability and meteorological variability of the sites. In conclusion, the noted values are found to be consistent, which indicate good calibration stability of INSAT-3DR VIS and SWIR channels.

Error Analysis and Budget

The calibration uncertainty in the reflectance-based approach has been discussed in the earlier work (Thome 2001; Slater et al. 1996). Recently, the uncertainty was reassessed and improved uncertainty in the reflectance-based approach is estimated ∼ ± 3% in the middle of the visible portion of the spectrum (Czapla-Myres et al. 2015). The simulated TOA radiance depends on many variables like atmospheric parameters, surface reflectance measurements, solar and viewing geometry, which directly affects the accuracy of the calibration exercises. The dependence

Table 3 Estimated uncertainty in the reflectance-based approach for VIS and SWIR channels of INSAT-3DR imager both for Day-1 and Day-56

Source of uncertainty	VIS (Day-1) (%)	SWIR (Day-1) (%)	VIS (Day-56) (%)	SWIR (Day-56) (%)
Surface reflectance measurements				
Spectralon panel calibration	1.6	1.6	1.6	1.6
Ground measurement errors	3.0	8.0	1.9	3.0
Absorption computation				
Total columnar ozone	1.5	1.5	1.5	1.5
Columnar water vapor	1.7	1.7	1.7	1.7
Optical depth measurements	1.2	1.2	1.2	1.2
Selection of aerosol type[a]	1.12	1.11	1.12	1.11
Uncertainty due to BRDF effect	1.2	1.75	0.52	0.88
Inherent code accuracy	0.6	0.6	0.6	0.6
Total uncertainty (root sum of squares)	4.60	8.82	3.82	4.52

[a]For the total uncertainty estimation, uncertainty due to selection of desert model only considered

of TOA radiance on these variables is complex and it is difficult to quantify it in a closed, analytical form.

(a) The important source of uncertainty is dominated by the laboratory determination of reference panel BRF. We have maintained the Spectralon diffuse reflectance standard, which is calibrated and traceable to the NIST. The recently estimated uncertainty in the panel measurement is ± 1.5%/1.7% in the VIS/SWIR region.

(b) The uncertainty on the mean field reflectance spectrum is due to variability in the surface characteristics. This uncertainty is estimated by calculating the standard error of the mean at each band for the mean filed reflectance spectrum. The mean relative errors are found to be 3 and 8% for Day-1 and 1.9 and 3% for Day-56 in VIS and SWIR bands respectively.

(c) In addition, the uncertainty is caused by the 6SV model. The estimated accuracy for 6SV RT code is much improved compared to the earlier version and the relative error is estimated as 0.4–0.6% (Kotchenova et al. 2008; Chen et al. 2014) according to the radiative transfer theory.

(d) In practise, it is difficult to accurately determine the aerosol properties in field experiments. In the present study, the aerosol type analysis confirms the selection of optimum aerosol model. Then again two other aerosol types (i.e. urban aerosols and desert aerosol) are chosen to replace the continental aerosol model in order to approximate their contributions to the systematic calibration uncertainty. We have re-calculated the calibration coefficients using 6SV RT code with different aerosol types. It is evident that the reflectance-based method is more sensitive to aerosol type than other methods. The relative errors are 1.12 and 1.11% for VIS and SWIR respectively, using desert aerosol model and 2.15%, and 2.14% for VIS and SWIR respectively, using urban aerosol model.

(e) The bi-directional reflectance distribution function (BRDF) effect is adding an uncertainty into calibration coefficient, which is one of the important steps in vicarious calibration. The effect of surface reflectance anisotropy was assessed by estimating TOA radiance with the BRDF coefficients (using MODIS BRDF product) for a site and comparing this with TOA radiance computed using surface measurements. The estimated uncertainty due to BRDF effect is 1.2 and 1.75% for Day-1 and 0.52 and 0.88% for Day-56 in VIS and SWIR respectively.

(f) The estimated uncertainty due to measurements of aerosol optical depth, total columnar ozone and columnar water vapor is 1.2, 1.5 and 1.7%, respectively.

From the uncertainty analysis (Table 3), the total uncertainty involved in the calibration coefficient is 4.60 and 8.82% for Day-1 and 3.82 and 4.52% for Day-56 in VIS and SWIR channels of INSAT-3DR, respectively.

Conclusion

In the present study, post-launch vicarious calibration was carried out for the VIS and SWIR channels of INSAT-3DR during Day-1 and Day-56 over GROK to monitor the radiometric performance of the sensors.

The conclusions are:

1. The radiometric performance of VIS channel was observed consistent since Day-1 to Day-56, whereas the large contribution of sub-surface soil moisture increases the uncertainty in the derived calibration coefficients of INSAT-3DR for Day-1. Furthermore, the noted values of calibration coefficients during Day-56 indicate the good laboratory calibration stability of both VIS and SWIR channels of INSAT-3DR imager.
2. Spatial variability of the site is quantified by the coefficient of variation (CV). The mean value of spatial CV is found 3.1 and 2.9% for VIS and 5.5 and 3.9% for SWIR on Day-1 and Day-56 respectively. These values indicate more uniformity of the calibration site during Day-56 compared to Day-1.
3. The 6SV simulated radiances are in good agreement with INSAT-3DR measured radiance for both the bands over GROK during Day-56.
4. Uncertainties in calibration coefficient due to selection of aerosol model are found to be 1.11–1.32% for desert model and 2.14–2.57% for urban model. Uncertainty due to BRDF effect is estimated using MODIS BRDF products, which was found to be 1.2 and 1.75% for Day-1 and 0.52 and 0.88% for Day-56 in VIS and SWIR respectively.
5. Estimated total uncertainty in computed calibration coefficient is found 4.60 and 3.82% for VIS and 8.82 and 3.52% for SWIR during Day-1 and Day-56, respectively.
6. The present study also concludes that GROK site is the preferred site for post-launch calibration due its spatial homogeneity, which helps to derive precise vicarious calibration coefficients.

Acknowledgements The authors gratefully acknowledge the encouragement received from Tapan Misra, Director, SAC for carrying out the present research work. Valuable suggestions received from Dr Raj Kumar, Deputy Director, EPSA is also gratefully acknowledged. Authors would like to thanks their respective families for their continuous motivations. The authors are grateful to anonymous reviewers for constructive and useful comments.

References

Badarinath, K. V. S., Kharol, S. K., Kaskaoutis, D. G., & Kambezidis, H. D. (2007). Dust storm over indian region and its impact on the ground reaching solar radiation—A case study using multi-satellite data and ground measurements. *Science of the Total Environment, 384,* 316–332.

Bannari, A., Omari, K., Teillet, P. M., & Fedosejevs, G. (2005). Potential of Getis statistics to characterize the radiometric uniformity and stability of test sites used for the calibration of Earth observation sensors. *IEEE Transactions on Geoscience and Remote Sensing, 43*(12), 2918–2926.

Bouvet, M. (2014). Radiometric comparison of multispectral imagers over a pseudo-invariant calibration site using a reference radiometric model. *Remote Sensing of Environment, 140,* 141–154.

Bruegge, C. J., Duval, V. G., Chrien, N. L., Korechoff, R. P., Gaitley, B. J., & Hochberg, E. B. (1998). MISR prelaunch instrument calibration and characterization results. *IEEE Transactions on Geoscience and Remote Sensing, 36,* 1186–1198.

Bruegge, C. J., Stiegman, A. E., Rainen, R. A., & Springsteen, A. W. (1993). Use of Spectralon as a diffuse reflectance standard for in-flight calibration of earth-orbiting sensors. *Optical Engineering, 32,* 805–814.

Chander, G., Xiong, X., Choi, T., & Angal, A. (2010). Monitoring on-orbit calibration stability of the Terra MODIS and Landsat 7 ETM+ sensors using pseudo-invariant test sites. *Remote Sensing of Environment, 114,* 925–939.

Chen, Z., Zhang, B., Zhang, H., & Zhang, W. (2014). Vicarious calibration of Beijing-1 multispectral imagers. *Remote Sensing, 6,* 1432–1450. https://doi.org/10.3390/rs6021432.

Cosnefroy, H., Leroy, M., & Briottet, X. (1996). Selection and characterization of Saharan and Arabian desert sites for the calibration of optical satellite sensors. *Remote Sensing of Environment, 58,* 101–114.

Czapla-Myres, J., McCorkel, J., Anderson, N., Thome, K., Biggar, S., Helder, D., et al. (2015). The ground-based absolute radiometric calibration of landsat 8 OLI. *Remote Sensing, 7,* 600–626. https://doi.org/10.3390/rs/0100600.

Frouin, R., & Gautier, C. (1987). Calibration of NOAA-7 AVHRR, GOES-5, and GOES-6 VISSR/VAS solar channels. *Remote Sensing of Environment, 22,* 73–101.

Gellman, D. I., Biggar, S. F., Slater, P. N., & Bruegge, C. J. (1991). Calibrated intercepts for solar radiometers used in remote sensor calibration. *Proceedings of SPIE, 1493,* 19–24.

Gu, X., Guyot, G., & Verbrugghe, M. (1990). Analyze de la variabilité spatiale d'un site-test: Exemple de "La Crau" (France). *Photo Interpretation, 1*(5), 39–52.

Kotchenova, S. Y., Vermote, E. F., Levy, R., & Lyapustin, A. (2008). Radiative transfer codes for atmospheric correction and aerosol retrieval: Intercomparison study. *Applied Optics, 47*(13), 2215–2226.

Markham, B. L., Halthore, R. N., & Goetz, S. J. (1992). Surface reflectance retrieval from satellite and aircraft sensors: results of sensor and algorithm comparison during FIFE. *Journal of Geophysical Research, 97*(D17), 18785–18795. http://dx.doi.org/10.1029/92JD02077.

MODIS ATBD, Strahler, A. H., & Muller, J. P. (1999). MODIS BRDF/Albedo Product, Algorithm Theoretical Basis Document, Version 6.

Morys, M., Mims, F. M., III, Hagerup, S., Anderson, S. E., Baker, A., Kia, J., et al. (2001). Design, calibration, and performance of MICROTOPS II handheld ozone monitor and Sun photometer. *Journal of Geophysical Research, 106*(D13), 14573–14582.

Nicodemus, F. E., Richmond, J. C., Hsia, J. J., Ginsberg, I. W., & Limperis, T. (1977). Geometrical considerations and nomenclature for reflectance, Natl. Bur. Stand. Rep. NBS MN-160, 52.

Patel, P., Bhatt, H., & Shukla, A. K. (2014). Absolute vicarious calibration of recently launched Indian meteorological satellite: INSAT-3D imager. ISPRS technical Commission VIII symposium, 09–12 December, 2014, Hyderabad, India. https://doi.org/10.5194/isprsarchives-XL-8-291-2014.

Patel, P., Bhatt, H., Mathur, A. K., Prajapati, R. P., & Tyagi, G. (2016). Reflectance-based vicarious calibration of INSAT-3D using high-reflectance ground target. *Remote Sensing Applications: Society and Environment, 3,* 20–35. https://doi.org/10.1016/j.rsase.2015.12.001.

Porter, J. N., Miller, M., Pietras, C., & Motell, C. (2001). Ship-based sun photometer measurements using microtops sun photo-

meters. *Journal of Atmospheric and Oceanic Technology, 18,* 765–774.

Rao, C. R. N. (2001). Implementation of the post-launch vicarious calibration of the GOES imager visible channel (Camp Springs, MD: NOAA Satellite and Information Services (NOAA/NESDIS)). http://www.ospo.noaa.gov/Operations/GOES/calibration/vicarious-calibration.html.

Reagan, J. A., Thomason, L. W., Herman, B. M., & Palmer, J. M. (1986). Assessment of atmospheric limitations on the determination of the solar spectral constant from ground-based spectroradiometer measurements. *IEEE Transactions on Geoscience and Remote Sensing., 24,* 258–266.

Rondeaux, G., Steven, M. D., Clark, J. A., & Mackay, G. (1998). La Crau: A European test site for remote sensing validation. *International Journal of Remote Sensing, 19*(14), 2775–2788.

Schmid, B., & Wehrli, C. (1995). Comparison of sun photometer calibration by use of the Langley technique and standard lamp. *Applied Optics, 34,* 4500–4512.

Scott, K. P., Thome, K. J., & Brownlee, M. (1996). Evaluation of the railroad valley playa for use in vicarious calibration. *Proceedings SPIE, 2818,* 158–166.

Slater, P. N., Biggar, S. F., Holm, R. A., Jackson, R. D., Mao, Y., Moran, M. S., et al. (1987). Reflectance-and radiance-based methods for in-flight absolute calibration of multispectral sensors. *Remote Sensing of Environment, 22*(11–37), 1987.

Slater, P. N., Biggar, S. F., Thome, K. J., Gellman, D. I., & Spyak, P. R. (1996). Vicarious radiometric calibrations of EOS sensors. *Journal of Atmospheric and Oceanic Technology, 13,* 349–359.

Teillet, P., & Chander, G. (2010). Terrestrial reference standard sites for post-launch sensor calibration. *Canadian Journal of Remote Sensing, 36,* 437–450.

Teillet, P. M., Horler, D., & O'Neill, N. T. (1997). Calibration, validation, and quality assurance in remote sensing: A new paradigm. *Canadian Journal of Remote Sensing, 23*(4), 401–414.

Thome, K. J. (2001). Absolute radiometric calibration of Landsat 7 ETM+ using the reflectance-based method. *Remote Sensing of Environment, 78,* 27–38.

Thome, K., Schiller, K. S., Conel, J., Arai, K., & Tsuchida, S. (1998). Results of the 1997 Earth Observing System Vicarious Calibration joint campaign at Lunar Lake Playa, Nevada (USA). *Metrologia, 35,* 631–638.

Vermote, E. D., Tanre, J. L., Deuze, M., Herman, J. J., Morcrette, & Kotchenova, S. Y. (2006). Second simulation of satellite signal in the satellite spectrum (6S). 6S User Guide Version 3. University of Maryland.